Laser and Particle Beams (2001), *19*, 181–186. Printed in the USA.

Relativistic laser interactions with preformed plasma channels and gamma-ray measurements

L.A. GIZZI,[1] M. GALIMBERTI,[1,2] A. GIULIETTI,[1] D. GIULIETTI,[1,2] P. TOMASSINI,[1]
M. BORGHESI,[3] D.H. CAMPBELL,[4] A. SCHIAVI,[4] AND O. WILLI[4]

[1]Intense Laser Irradiation Laboratory—IFAM, Area della Ricerca—CNR, Pisa, Italy
[2]Dipartimento di Fisica, Università di Pisa and INFM, Pisa, Italy
[3]Department of Pure and Applied Physics, The Queen's University, Belfast BT7 1NN, United Kingdom
[4]Imperial College of Science, Technology and Medicine, SW7 2BZ, London, United Kingdom

(RECEIVED 24 January 2000; ACCEPTED 5 February 2001)

Abstract

The propagation of a 1-ps laser pulse at intensities exceeding 10^{19} Wcm^{-2} in a low-density plasma channel was experimentally tested. The channel was produced by a lower intensity preceding pulse of the same duration. Plasma electrons were accelerated during the propagation of the main pulse, and high energy γ-ray detectors were used to detect their bremsstrahlung emission. The γ-ray yield was studied for different channel conditions, by varying the delay between the channel forming pulse and the high intensity pulse. These results are correlated with the interferograms of the propagation region into the plasma.

1. INTRODUCTION

The advent of lasers in the chirped pulse amplification (CPA) mode allowed for the first time the interaction of ultra-short radiation pulses with plasmas at relativistic intensities to be achieved. The very large electric fields of such pulses can accelerate, directly or via induced perturbations of the electron density, charged particles (Borghesi, *et al.*, 1999; Gremillet *et al.*, 1999; Krushelnick *et al.*, 1999; Pukhov *et al.*, 1999; Cowan *et al.*, 2000; Ledingham *et al.*, 2000). Depending on the plasma density, several mechanisms can be activated which accelerate electrons to much higher energies than those due to the laser ponderomotive potential. Stimulated Raman forward scattering (SRFS) and self-modulated laser wake-field acceleration (SMLWFA) are some of the mechanisms proposed to explain the generation of a large number of $>$10 MeV electrons in recent experiments (Tajima & Dawson, 1979; Tzeng *et al.*, 1997; Amiranoff *et al.*, 1998; Esarey *et al.*, 1998; Borghesi *et al.*, 1999; Gremillet *et al.*, 1999; Pukhov *et al.*, 1999). Theoretical studies also predict that energy conversion into energetic electrons should be favored when the laser pulse propagates in a cavitated structure such as a plasma channel. These issues may have important consequences on laser-driven plasma-based accelerators as well as on inertial fusion energy (IFE), particularly in the Fast Ignitor (FI) scheme. A major problem of laser-driven plasma-based accelerators is the short acceleration distance, which is basically limited by laser beam diffraction (Leemans *et al.*, 1998). Propagation in a plasma channel has been proposed as a way of overcoming this limitation. It is well established that channels can be produced (Borghesi *et al.*, 1997; Malka *et al.*, 1997) as a result of laser interaction with underdense plasmas. Several experiments (Krushelnick *et al.*, 1997; Wagner *et al.*, 1997; Mackinnon *et al.*, 1998, 1999) have also demonstrated that efficient guiding of ultraintense pulses in a channel is indeed possible. From the point of view of the fast ignitor approach to inertial fusion, the occurrence of nonponderomotive acceleration mechanisms typical of the ultraintense regime may result in a loss of energy if the stopping range of these electrons is much greater than the typical size of the compressed core of an IFE pellet. It is therefore important to assess the role of these additional acceleration mechanisms and their importance in the energy balance.

Fast electrons generated in laser-plasma interactions at relativistic intensities can be studied directly using electron spectrometers, or indirectly, detecting the γ-ray bremsstrahlung radiation generated by the interaction of these electrons with matter. The γ-ray detection technique is particularly suitable when the energy of the fast electrons is expected to be very high ($\gg$10 MeV) and usual magnetic electron spectroscopy would require dedicated, large scale equipment.

Address correspondence and reprint requests to: Marco Galimberti, Istituto di Atomica e Molecolare, Area della ricerca, via Alfieri 1, 56010 Ghezzano, Pisa, Italy.

Here we report on a recent investigation carried out at the Vulcan laser facility, Rutherford Appleton Laboratory (United Kingdom) in which γ-ray detection was employed to study the effect of a precursor channeling pulse on the electron acceleration obtained with the main Vulcan CPA laser pulse (75 J, 1 ps, 1.054 μm) in an underdense plasma. The electrons were converted via bremsstrahlung into γ-rays, basically when the beam of accelerated electrons collided with massive components present along its path in the vacuum chamber where the laser plasma interactions took place. The γ-ray yield was monitored for different conditions of the preformed channel by varying the delay between the channel forming pulse and the main CPA pulse.

2. EXPERIMENTAL SETUP

The layout of the experimental arrangement has been published elsewhere (Galimberti *et al.*, 2000). The plasma was produced by using a well-established technique (Gizzi *et al.*, 1994) based upon the explosion of thin plastic foils (0.1, 0.3, or 0.5 μm thick) by two 600 ps, 0.527 μm Vulcan laser pulses at a total irradiance of about 5×10^{14} W/cm^2. After a suitable delay (typically of the order of 1 ns), the main CPA pulse was focused into the plasma. At this time the peak density of the plasma was below $n_c/10$ and its longitudinal extent was of the order of 1 mm. With an f/3.5 focusing optics, the irradiance "in vacuum" of the main CPA pulse was up to 5×10^{19} W/cm^2 (about 50 J on target, with up to 50% of the energy in a 10–15 μm focal spot). A fraction of the energy of the main CPA pulse was used to provide a prepulse, collinear with the main pulse. The prepulse could be focused into the preformed plasma before the main pulse and used to dig a density channel. The delay Δt between the channel forming pulse and the main pulse ranged from 20 to 120 ps in the data set discussed in this paper. A further small fraction of the CPA pulse was frequency quadrupled and used as a transverse optical probe reaching the channel with a fixed delay of 5 ps after the propagation of the main pulse through the plasma. Interferometry was performed with the probe in a modified Nomarsky configuration (Benattar *et al.*, 1979). The relative timing of the four pulses (for heating, channel formation, propagation, and probing, respectively) is shown in Figure 1. For the data discussed in this paper, only the channel formation to propagation time Δt was varied. Other diagnostics included calorimetry of the energy transmitted through the plasma, imaging of the transmitted laser spot, and forward- and back-scatter spectroscopy.

A set of photomultipliers coupled with scintillating crystals (thickness ranging from 12.5 to 50.1 mm) was placed along the direction of the transmitted CPA pulse while two additional 50.1-mm detectors were placed at 45° and 90°, respectively. All scintillators were shielded from side-scattered radiation by a 50-mm lead case. Lead slabs were also used to reduce the signal below the PM saturation level. According to numerical simulations performed using the code GEANT4 (GEANT4, 1998), the total mass density placed along the line of view of the detectors ensures that primary electrons with energy up to several hundred megaelectronvolts do not reach the detectors. As electrons of such a level of energy are very unlikely to be produced, we can assume that the signal of the scintillators is mostly due to γ-ray photons generated by bremsstrahlung of primary electrons.

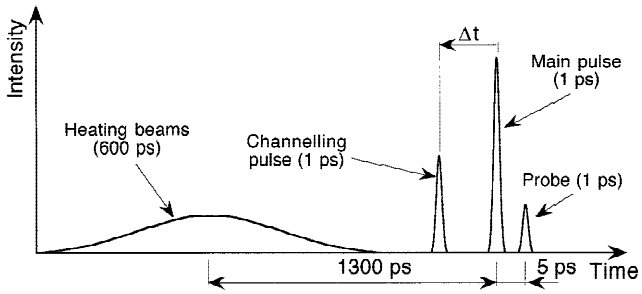

Fig. 1. Timing of the four laser pulses involved in the experiment. Pulse shapes and delays are not in scale.

3. RESULTS AND DISCUSSION

A preliminary survey (Galimberti *et al.*, 2000) of the data indicates that a large number of very high-energy electrons were generated mostly in the forward direction by the CPA laser pulse propagating through the preformed plasma channel. Assuming a given direction of the primary electrons (i.e., the direction of propagation of the main laser pulse), the comparison of simulations with the experimental data obtained from the scintillators allows a correlation to be established between the number of electrons and their energy. The properties of the primary electron beam from which γ-rays originate have been reconstructed using a Monte Carlo simulation code. This simulation indicates that the "mean" energy of individual electrons must be >10 MeV for a large number of electrons (up to a number of the order of 10^{13}).

A γ-ray signal was also observed when the high intensity CPA pulse directly interacted with the plasma, without any preliminary formation of the channel. In this case, however, the signal was found to be extremely variable shot-to-shot. Correspondingly, the interferograms taken 5 ps after the main pulse propagation showed clear evidence for laser beam break-up and formation of filaments (Galimberti *et al.*, 2000).

Much more reproducible data were obtained in the case of CPA pulse propagation in the preformed channel. They showed an interesting trend of the γ-ray signal to increase when the delay between the channel formation and the arrival of the main pulse on the plasma increased from 20 to 120 ps. To better discuss this effect, in this paper we will restrict ourselves to a homogeneous set of data, namely those obtained with targets of 0.3 μm thickness at the main

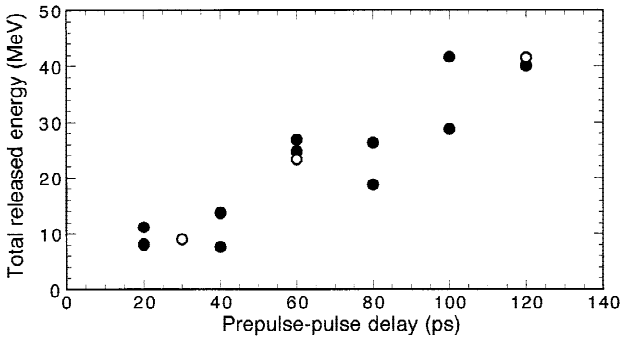

Fig. 2. Energy released by the gamma-ray photons to the detector set versus the delay Δt between the channel forming pulse and the main CPA pulse. The data were obtained with 0.3-μm plastic targets, and timing as indicated in Figure 1. The nominal irradiance of the main CPA pulse was 3×10^{19} W/cm^2.

pulse nominal irradiance of 3×10^{19} W/cm^2. Excluding Δt, all the other experimental parameters are fixed, including the intensity of all the laser pulses (devoted to the plasma creation and channel formation) and the delay of the probe pulse (5 ps after the propagation of the main pulse).

The trend of the γ-ray signal is shown in Figure 2, where the total γ-ray energy released in the detectors is plotted versus the prepulse-pulse delay Δt for 14 homogeneous events performed with 0.3 plastic targets in the fixed experimental conditions stated above. There is a factor of four increase of the γ-ray yield when the delay between the plasma formation and the main pulse arrival goes from 20 to 120 ps. Correspondingly, the transmission rate of the main pulse after propagation through the channel increases more than six times (Borghesi *et al.*, 2001).

As described in the previous section, simultaneous interferograms have been produced to monitor plasma channeling and the modifications induced on the preformed plasma density by the CPA interaction pulse. In Figure 3, three of those interferograms are shown, corresponding to the three γ-ray data indicated by empty circles in Figure 2. The three interferograms were obtained for three different delays Δt, but the same delay from the plasma formation time. They represent, then, the fringe pattern produced by: (1) the channel evolution and (2) the propagation of the main pulse. Referring to the interferograms of Figure 3, the laser pulses come from the left-hand side. The Nomarsky technique we have used allows us to investigate both the entrance and exit sides of the original target.

The first interferogram (top picture of Fig. 3) shows the pattern for $\Delta t = 30$ ps. Qualitatively, there is evidence that, though the channel is already well defined, important fringe perturbations are present inside the channel, particularly in the higher density region close to the original target position. There is also evidence that the prepulse forming the channel loses its energy content while propagating through the plasma (consistently, the transmission of the prepulse energy through the plasma is basically zero). The energy transferred to the ions in the Coulomb explosion process (Borghesi *et al.*, 1998) is therefore smaller in the higher density region close to the original target position than in the low density entrance plasma. This determines a less efficient, slower expansion and the presence of turbulent structure in the early stages of the channel expansion. As a matter of fact, in shots where only the preforming channel pulse is present, no evidence of channel formation at the back side of the target was collected. For 30-ps delay, the transmission rate is still low (13% in our case), though definitely higher than the transmission for $\Delta t = 20$ ps (6%; Borghesi *et al.*, 2001). There is little evidence for the pulse transmission in the exit portion of the channel (right-hand side of the interferogram). Another important feature is the fringe blurring at the channel boundary, which is likely to be a combined effect of the fast channel expansion and of refraction due to the steep density gradients.

The second interferogram (middle picture of Fig. 3) shows the pattern for $\Delta t = 60$ ps. The channel has a large diameter, but is still expanding (fringe blurring). The channel entrance is less perturbed, but there is a clear evidence of filamentary and rather chaotic structures at the exit of the channel. Also in this case there is an analogy with observations performed after direct irradiation of the plasma by the main pulse (Galimberti *et al.*, 2000; Borghesi *et al.*, 2001). Our interpretation is that, although the channel appears considerably more homogeneous than in the previous case, the channel is well developed only in the front region of the plasma. The main pulse is then guided up to the central region of the plasma, where it has to dig its own channel, spending a considerable fraction of its energy and undergoing beam break-up and filamentation. Correspondingly, the transmission increases to 19%.

The third interferogram (bottom picture of Fig. 3) shows the pattern for $\Delta t = 120$ ps. Fringe blurring at the channel boundary is no longer present, indicating a channel in a quasi-stationary state. The transmission reaches about 38%. The channel region shows a quite regular fringe pattern. The rear side portion of the fringe pattern was lost in this shot.

A more quantitative study of the channel evolution has been done by analyzing the interferograms with a novel numerical tool (IACRE) which makes an extensive use of the Continuous Wavelet Transforms (Tomassini *et al.*, 2001). This technique is much more powerful than the standard FFT-based one (Gizzi *et al.*, 1994 and references therein) in two main aspects: it is *more robust* since it can be successfully used in analyzing poor-quality interferograms and *more accurate* since its sensitivity in the phase-shift estimation is higher than the one of the FFT-based method. In particular the IACRE technique was proved to be very effective in detecting small scale perturbations.

With this technique, the phase-shift maps of suitable portions of the two interferograms of Figure 3 are obtained. They are then (whenever it is possible) symmetrized with respect to the axis with an algorithm which optimizes the

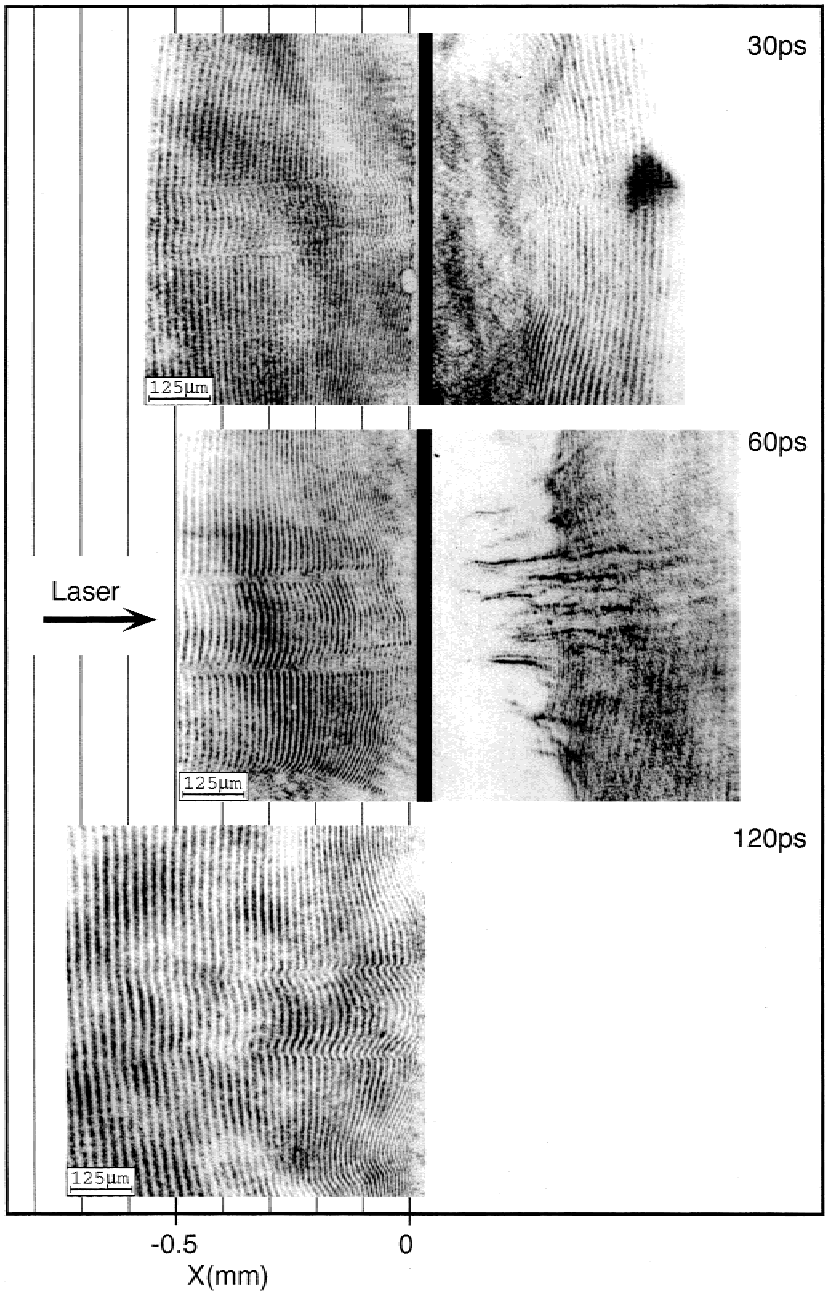

Fig. 3. Interferograms obtained (with 0.3-μm plastic targets, and timing as indicated in Fig. 1) by ultraviolet transversal probing of the channel, 5 ps after the propagation of the main pulse. Top: $\Delta t = 30$ ps, main pulse transmission through the plasma, 13%. Middle: $\Delta t =$ 60 ps, transmission 19%. Bottom: $\Delta t = 120$ ps, transmission 38%.

matching between the two half-maps. Finally, density maps are computed via Abel inversion. However, in some regions the fringe deviation from symmetry is so large that symmetrization is not justified.

The IACRE method has been applied to the fringe patterns obtained for $\Delta t = 30$ and 120 ps (top and bottom of picture of Fig. 3, respectively). In the case of $\Delta t = 120$ ps, the level of symmetry was quite high, allowing us to produce a density map of the whole channel region in front of the target, which appears in the top-left picture of Figure 4. The channel density profiles appear regular and smooth both longitudinally, along the axis (bottom left of Fig. 4), and transversally. The transverse profile is shown at two different positions along the channel, at the entrance ($x = -450$ μm, picture top right of Fig. 4) and closer to the original target position ($x = -100$ μm, picture bottom right of Fig. 4). In Figure 4 and Figure 5, $x = 0$ approximately corresponds to the original target position.

In the case of $\Delta t = 30$ ps, the level of symmetry was acceptable only at the entrance of the channel. The density map obtained in that region is shown in the top-left picture of Figure 5. At the bottom of the same figure, longitudinal

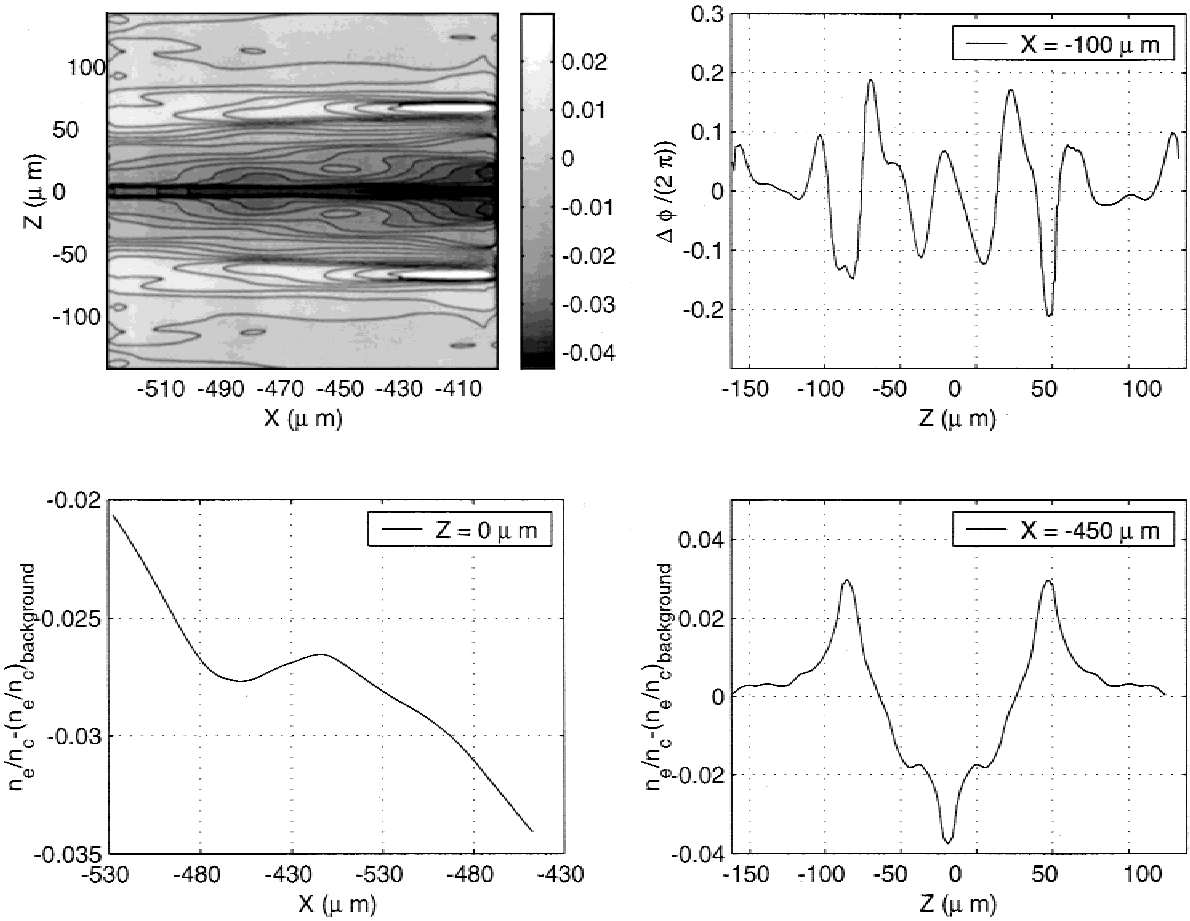

Fig. 4. Electron density distribution in the channel region inferred from the interferogram $\Delta t = 120$ ps (bottom of Fig. 3). The density is calculated relative to the background density profile for a given value of the x coordinate. Top left: the symmetrized density map; notice that the z-axis is expanded with respect to the x-axis one. Bottom left: longitudinal line-out of the density along the channel axis. Top right: transversal line-out of the phase shift taken at $x = -100$ μm. Bottom right: transverse line-out of the density taken at $x = -450$ μm. $x = 0$ corresponds approximately to the original target position.

on-axis and transverse (at $x = -450$ μm) line-outs of the same region are shown. In the remainder of the interferogram, the phase shift map evidenced a filamentary and rather chaotic structure, as provided by the transverse line-out of the phase shift taken at $x = -100$ μm (top right of Fig. 5). At this time, after the channel formation, the channel density profile appears to be unsuitable for the main pulse propagation a few hundred micrometers from its entrance.

The interpretation and analysis of the data are presently in progress. Eventually, computational modeling of the laser propagation in the plasma conditions corresponding to the various channeling-propagation delays will be required. However from this preliminary survey of the data, it appears that the presence of the channel determines a clear transition from a chaotic and unstable acceleration regime, dominated by filamentation and laser beam break-up (Young & Bolton, 1996; Wang *et al.*, 2000), to more controllable experimental conditions. The efficiency of the acceleration process increases as the channel interior becomes smoother, and the main pulse propagates in an uniform low-density plasma with gently rising edges.

In conclusion, the comparative analysis of γ-ray yield and interferograms, performed on an homogeneous set of data, shows that the technique used to preform a density channel in the plasma may be effective to accelerate electrons with very intense laser pulses of 1 ps duration. As a matter of fact, a large number of electrons were to be accelerated forward to ultrarelativistic energies. However the status of evolution of the channel seems to play a major role in the efficiency of the acceleration process. In the experimental conditions of the data we have studied, the energy collected by the γ-ray detectors, which is proportional to the sum of the individual electron energies, increased with the delay between the channel forming pulse and the accelerating pulse. Though longer delays were not investigated, a delay of the order of 100–120 ps gave evidence for efficient acceleration corresponding to a rather stationary status of the channel in the time scale of the accelerating pulse propagation (a few picoseconds). The interferograms also suggest that for the given plasma parameters, a channel was fully formed only on the front side of the plasma. This is obviously detrimental to an efficient propagation of the accelerating pulse.

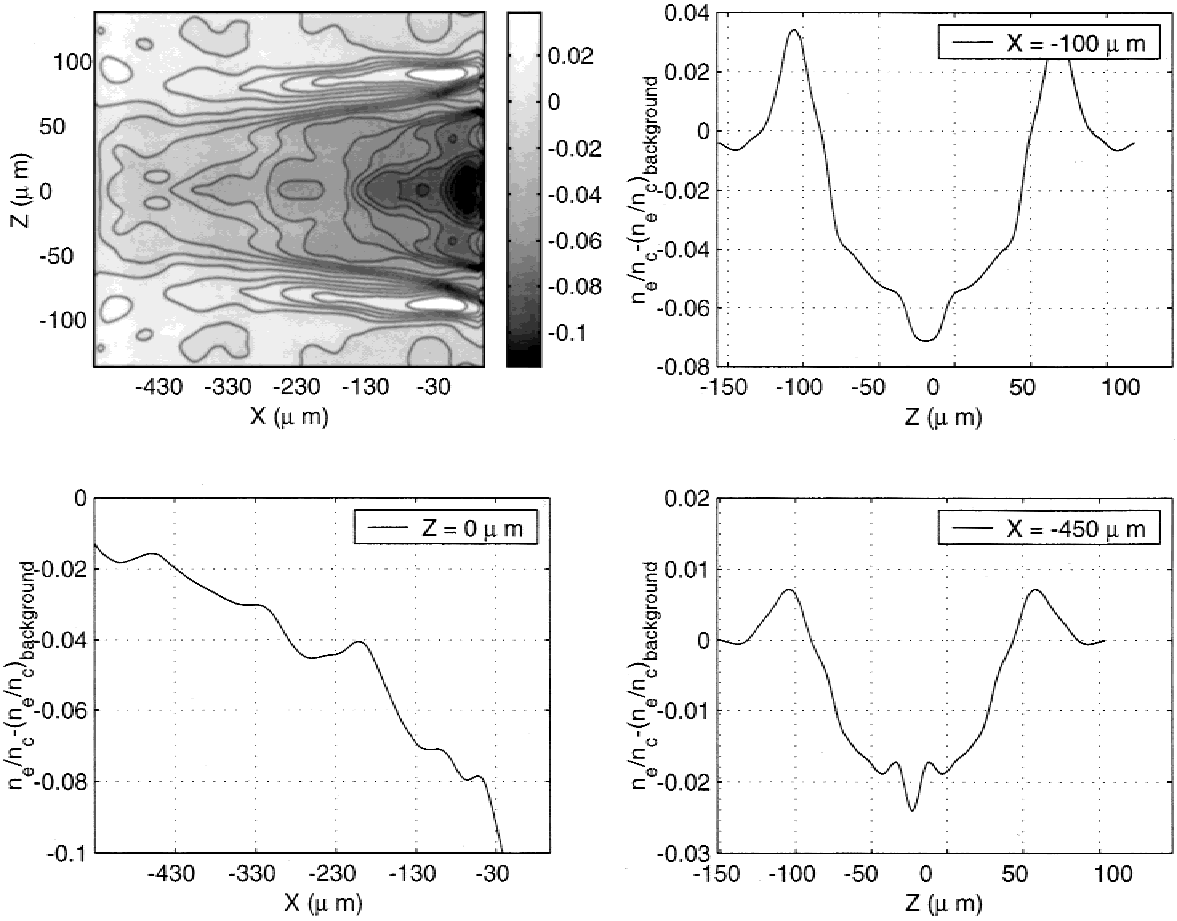

Fig. 5. Numerical analysis of the channel region inferred from the interferogram $\Delta t = 30$ ps (top of Fig. 3). Top left: the symmetrized electron density map of the entrance region, after subtraction of the background density profile. Bottom left: longitudinal line-out of the density along the channel axis. Top right: transverse line-out of the density taken at $x = -100$ μm. Bottom right: transverse line-out of the density taken at $x = -450$ μm. $x = 0$ approximately corresponds to the original target position.

ACKNOWLEDGMENTS

We thank the staff of the Central Laser Facility at RAL for their enthusiastic support in preparing and carrying out the experiment. We also thank A. Barbini (IFAM-CNR) for his contribution to the experimental setup. One of the authors (P.T.) acknowledges financial support from M.U.R.S.T. (Project: "Metodologie e diagnostiche per materiali e ambiente"). The experiment was funded by an ESPRC grant. Also, the authors wish to acknowledge support from the Training and Mobility of the Researchers European Network, involved in the project "X-ray Probing of Matter" (XPOSE, contract No. HPRNT2000-00160).

REFERENCES

Amiranoff, F. *et al.* (1998). *Phys. Rev. Lett.* **81**, 995.
Benattar, R., Popovics, C. & Siegel, R. (1979). *Rev. Sci. Instrum.* **50**, 1583.
Borghesi, M. *et al.* (1997). *Phys. Rev. Lett.* **78**, 879.
Borghesi, M. *et al.* (1998). *Phys. Rev. Lett.* **80**, 5137.
Borghesi, M. *et al.* (1999). *Phys. Rev. Lett.* **83**, 4309.
Borghesi, M. *et al.* (2000). *Laser Part. Beams* **18**, 1.
Borghesi, M. *et al.* (2001). **RAL-TR-2000-034** Rutherford Appleton Laboratory.
Cowan, T.E. *et al.* (2000). *Phys. Rev. Lett.* **84**, 903.
Esarey, E. *et al.* (1998). *Phys. Rev. Lett.* **80**, 555.
Galimberti, M. *et al.* (2000). *XXVI Eclim Conference, SPIE Proceedings.*
Geant4: LCB Status Report/**RD44**, 1998 CERN/LHCC-98-44.
Gizzi, L.A. *et al.* (1994). *Phys. Rev. E* **49**, 5628.
Gremillet, L. *et al.* (1999). *Phys. Rev. Lett.* **83**, 5015.
Krushelnick, K. *et al.* (1997). *Phys. Rev. Lett.* **78**, 4047.
Krushelnick, K. *et al.* (1999). *Phys. Rev. Lett.* **83**, 737.
Ledingham, K.W.D. *et al.* (2000). *Phys. Rev. Lett.* **84**, 899.
Leemans, W.P. *et al.* (1998) *Phys. Plasmas* **5**, 1615.
Malka, V. *et al.* (1997). *Phys. Rev. Lett.* **79**, 2979.
Mackinnon, A.J. *et al.* (1998). *Phys. Rev. Lett.* **80**, 5349.
Mackinnon, A.J. *et al.* (1999). *Phys. Plasmas* **6**, 2185.
Pukhov, A. *et al.* (1999). *Phys. Plasma* **6**, 2847.
Tajima, T. & Dawson, J.M. (1979). *Phys. Rev. Lett.* **74**, 267.
Tomassini, P. *et al.* (2001) submitted to *Applied Optics*.
Tzeng, K.C. *et al.* (1997). *Phys. Rev. Lett.* **79**, 5258.
Young, P.E. & Bolton, P.R. (1996). *Phys. Rev. Lett.* **77**, 4556.
Wagner, R. *et al.* (1997). *Phys. Rev. Lett.* **78**, 3125.
Wang, X. *et al.* (2000). *Phys. Rev. Lett.* **84**, 5324.